Energy Storage System as Auxiliaries of Internal Combustion Engines in Hybrid Electric Ships

Seungwan Nam
Engine Control Engineering Dep't
Hyundai Heavy Industries Co., Ltd.
Ulsan, Republic of Korea
Email: nswan@hhi.co.kr

Daeseong Park
Department of Marine Technology
Norwegian University of Science and Technology
Trondheim, Norway
Email: daeseong.park@ntnu.no

Mehdi Karbalaye Zadeh
Department of Marine Technology
Norwegian University of Science and Technology
Trondheim, Norway
Email: mehdi.zadeh@ntnu.no

***Abstract*— This paper presents a design concept to overview the feasibility of utilizing modern energy storage systems as substitution of conventional machinery auxiliaries, which are necessarily installed to support internal combustion engines' operation. For example, the common compressed air system required for engine starting and emergency stopping occupies substantial space in the machinery space of the ship. Owing to increased capacity and reduced price of batteries nowadays, electric motors and solenoid valves can supersede the compressed air system, and we can save space and reduce capital expenditures as well. The cranking torque for engine starting, motor driving current, the optimal control system is simulated to validate the performance of the engine starting system, in line with the simulation of charging and discharging of an energy storage system.**

Keywords—Engine starting system, battery management system, Transportation electrification, DC motor control, DC-DC converter, Energy Storage System, Hybrid ships

I. INTRODUCTION

Recent developments of power electronics and energy storage systems drive transportation industries moving to pure electrification. [1]. However, it is unlikely to exclude conventional internal combustions engines, i.e., diesel and gas-fueled engines for vessels with medium to long sailing distances, heavily loaded cargos, and operation with dynamic positioning. Mostly, engines for those kinds of vessels, basically, equipped with a compressed air system, which dedicated to starting and controlling engines. Compressed air system for engine starting, comprised with an air compressor, air tank, relevant pipes, and air motor is represented in Fig.1 If we replace the compressed air system with the electric energy storage system (ESS), the system can be minimized as shown in Fig. 2.

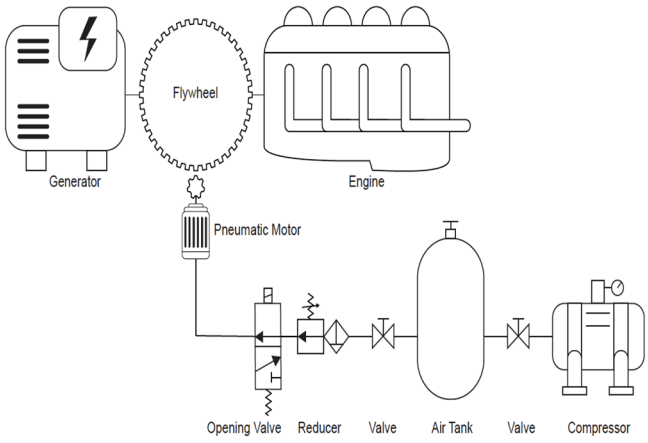

Fig. 1. Compressed air system for engine starting and control

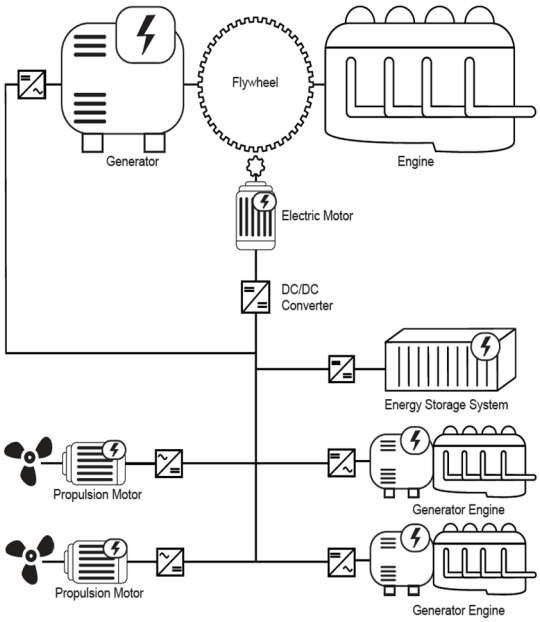

Fig. 2. Proposed engine starting system in a hybrid ship

Instead of the air starting motor, an electric motor, preferably a DC motor can be used for engine starting, in consequence, the air compressor and air tank to be replaced by an electric energy source, mostly equipped in hybrid electric ships. It will result in cost and space-saving in the engine room, as the air compressor is bulky and expensive. In this scheme, the electric power is supplied by the main energy system of the hybrid ship, hence, no separate ESS is needed.

This paper presents the design concept to investigate the feasibility of using DC electric motor and the hybrid ship's ESS to replace the conventional machinery for the engine auxiliaries. It includes modeling, design, and control of the DC motor and ESS. The ESS is connected to the DC motor through a Buck-Boost DC-DC converter, constituting a local DC microgrid. Simulation results are given in Section IV to verify the performance of the electric auxiliary system.

II. MODELLING OF STARTING MOTOR AND BATTERY

A. Engine Cranking Torque and Speed

A generator engine, which is a rotating machine, can be therefore given its dynamic characteristic by [2]:

$$J_m \dot{\omega}_m = \sum T_i \qquad (1)$$

where J_m is the moment of inertia sum of engine and generator, ω_m is the angular velocity of engine, and T_i are torques applied to engine crank shaft.

The equation can be converted to per unit (pu) by defined inertia constant H [2]:

$$H = \frac{J_m \omega_{m,b}^2}{2P_b} = \frac{J_m \omega_{m,b}}{2T_b} \quad (2)$$

Equation (1) now can be converted to:

$$2\frac{H\dot{\omega}_m}{\omega_{m,b}} = 2H\dot{\omega} = \sum \frac{T_i}{T_b} = \sum t_i \quad (3)$$

where $\omega = \frac{\omega_m}{\omega_{m,b}}$ is the per unit angular velocity, $t_i = \frac{T_i}{T_b}$ is the per unit torque, P_b is the base power of the generator set, and T_b is the base torque.

Now, engine speed can be expressed with each torque applied to engine crank shaft:

$$\dot{\theta} = \omega\omega_b \quad (4)$$

$$\dot{\omega} = \frac{1}{2H}(-D_f\omega + \tau_m - \tau_e) \quad (5)$$

where θ is the mechanical angle, D_f is the damping due to friction and windage of engine compartments torque from generator [3].

Be noted that during engine starting, there is no ignition generated in engine cylinder chambers, thus, τ_m is the torque only from the electric starting motor, and the generator does not provide electric power in the engine starting phase, τ_e is zero, accordingly, the equation can be simplified as:

$$\dot{\omega} = \frac{1}{2H}(-D_f\omega + \tau_m) \quad (6)$$

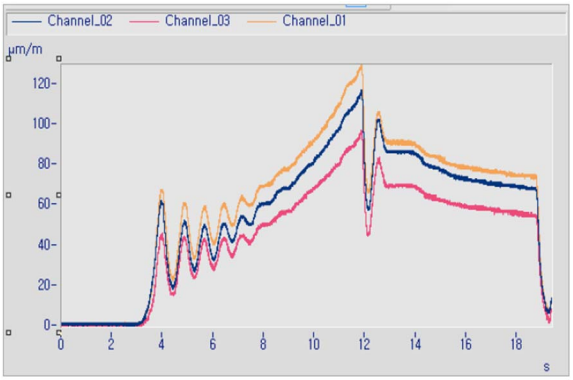

Fig. 3. Strain measurement for turning HiMSEN 20H35DFV

The actual cranking torque was measured from a 4-stroke dual-fuel engine, Hyundai Himsen 20H35DFV. The torque for rotating the engine is estimated by strain measurement while turning the engine with 60 degrees in 15 seconds, i.e., $\frac{2}{3}\ rpm$.

The maximum stress measured was 23.8 MPa, it is estimated that 29.8 kN force was required for engine turning. It is given that the total inertia of the engine and generator is $4{,}033.7 kg \cdot m^2$ and the base power is 9,600kW. The inertia constant is calculated as:

$$H = \frac{4033.7\times(720\cdot\frac{2\pi}{60})^2}{2\times9600\times10^3} = 1.194,$$

and assuming $D_f = 1, \dot{\omega} = \frac{2}{3}\times\frac{2\pi}{60}/0.5, \omega = \frac{2}{3}\times\frac{2\pi}{60}$ the per unit torque can be calculated by the equation (6) and the result is $\tau_m = 0.235\ pu$.

Now we can derive the require torque to of the motor from the calculation, $\tau_m = \frac{T_{motor}}{T_b} = \frac{T_{motor}\cdot\omega_{m,b}}{P_b} = \frac{T_{motor}\cdot720\cdot\frac{2\pi}{60}}{9600} = 0.23\ pu$,

accordingly, the value of the torque is

$$T_{motor} = \frac{0.235\cdot9600\cdot10^3}{720\cdot\frac{2\pi}{60}} = 29.92 \text{ kN}.$$

It is noted that measured torque and torque calculated by the model are similar. Thus, in this paper, the torque reference of the motor will be generated by equation (6), where we assume the damping constant, due to friction and windage as $D_f = 1$.

For 4-stroke engines, it normally takes 15~20 seconds to reach their rated speed and takes 5 seconds to reach the cranking speed by starting motor. After the engine reaches 150 rpm, fuel ignition in each cylinder powers the engine to rotate, and the engine speed will be controlled by the governor, which regulates the fuel injection amount to each cylinder. In this paper, 5 seconds to reach 150 rpm is used for the speed reference, and the starting motor speed will be controlled by Buck converter by controlling voltage and current of DC motor to follow the speed reference during the starting period.

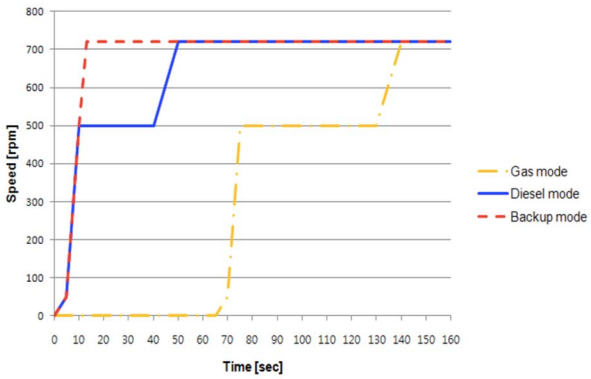

Fig. 4. 4-stroke engine starting curve of HiMSEN H35DF

B. *Starting Motor*

To have a more efficient way of integration with onboard ESS and DC grid, a DC motor is applied for the engine starting system. To drive the engine to the cranking speed limit where fuel ignition begins to take place, the electric motor must have sufficient torque higher than the motoring torque of the engine. If a single motor is not enough to drive the engine, it is considerable to install multiple motors as Fig. 5.

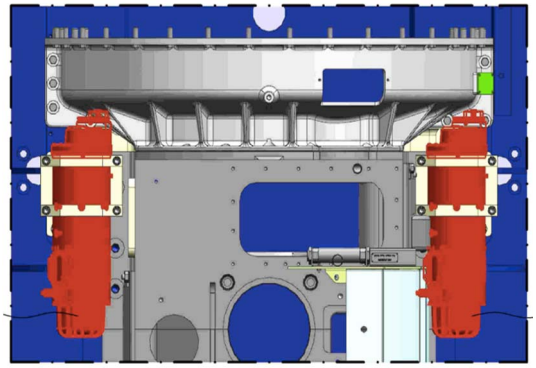

Fig. 5. Installation of two electric motors on engine flywheel cover

The field circuit and armature circuit of DC motor are modeled as [4]:

$$U_a = R_a I_a + L_a \frac{dI_a}{dt} + \omega \Psi_{af} \quad (7a)$$

$$\Psi_{af} = L_{af} I_f \, , E = \omega \Psi_{af} \quad (7b)$$

$$U_f = R_f I_f + \frac{d\Psi_f}{dt} \quad (8a)$$

$$\Psi_f = L_f I_f \quad (8b)$$

$$T_e = p \Psi_{af} I_a \quad (9)$$

where U_a is the armature voltage, R_a is the armature resistance, I_a is the armature current, L_a is the armature inductance, ω is the angular velocity [rad/sec], Ψ_{af} is the flux linkage in armature circuit due to the field winding, E is back emf, U_f is the field voltage, R_f is the field winding resistance, I_f is the field current, Ψ_f is the flux linkage in field circuit, L_f is the field inductance, p is number of poles, and T_e is the output torque of the motor.

The equations can be converted to per unit (pu) as well by definition of pu-quantities and parameters [4]:

$$u_a = r_a i_a + l_a \frac{di_a}{dt} + n \cdot \mathrm{i}_f \quad (10a)$$

$$\psi_{af} = l_{af} \cdot i_f = i_f \quad (10b)$$

$$u_f = i_f + T_f \frac{di_f}{dt} \quad (11a)$$

$$\psi_f = l_f \cdot i_f = l_{af} \cdot i_f = i_f \quad (11b)$$

$$\tau_e = \psi_{af} \cdot i_a = i_f \cdot i_a \quad (12)$$

where $u_a = \frac{U_a}{U_{a,base}}$ is the per unit armature voltage, $i_a = \frac{I_a}{I_{a,base}}$ is the per unit armature current, l_a is the per unit armature inductance, $n = \frac{\omega}{p \cdot \Omega_{base}} = \frac{\Omega}{\Omega_{base}}$ is the per unit speed, ψ_{af} is the per unit flux linkage in armature circuit due to the field winding, u_f is the per unit field voltage, i_f is the per unit field current, $T_f = \frac{L_f}{R_{fN}}$ is the time constant of the field circuit, and τ_e is the per unit output torque of the motor. Neglecting the magnetic saturation and temperature increase, we assumed that $r_f = 1$ and $l_{af} = 1$.

C. Buck-Boost Converter

The ESS in the vessel will feed the motor power. A buck-boost converter can be applied for a hybrid DC microgrid [4] and also for motor drive. The pu-model for the armature circuit and field circuit can be modeled as [4]:

$$u_a = u_{dc} \cdot u_{control}(t - T_{delay}) \quad (13)$$

$$u_f = u_{dc,f} \cdot u_{control,f}(t - T_{delay,f}) \quad (14)$$

where $u_{dc} = \frac{U_{dc}}{E_{aN}}$ is the per unit source voltage, $u_{control}$ is the control signal (modulation index) in buck converter, and $T_{delay} = \frac{T_{sw}}{3}$ is the time delay in the converter.
Now, the the circuit can be represented as Laplace form:

$$i_a(s) = \frac{u_{dc} \cdot e^{-s \cdot T_{delay}} \cdot u_{control}(s) - n(s) \cdot i_f(s)}{r_a \cdot (1 + T_a \cdot s)} \quad (15)$$

$$i_f(s) = \frac{u_{dc,f}}{(1 + T_f \cdot s)} \cdot e^{-s \cdot T_{delay}} \cdot u_{control}(s) \quad (16)$$

As presented equation (12), the motor torque depends on the armature current and field current, and according to (10), the motor speed is related to armature voltage, armature current, and field current.

The control schemes using DC to DC Buck converter to driving DC motor are presented through several studies [6 ~ 13]. In this paper, a Buck converter is used to control the speed and torque of the DC motor by controlling the armature voltage and current. We assume that the field current and voltage are constant in the model to examine the effect of armature voltage and current, and this strategy also can be applied for permanent magnet DC motor. The desired voltage and current are controlled by the duty cycle, which is computed by a proportional-integral (PI) controller. Both speed error and torque error are summed and fed to the PI controller, therefore, Buck converter can control both the voltage and current of the armature.

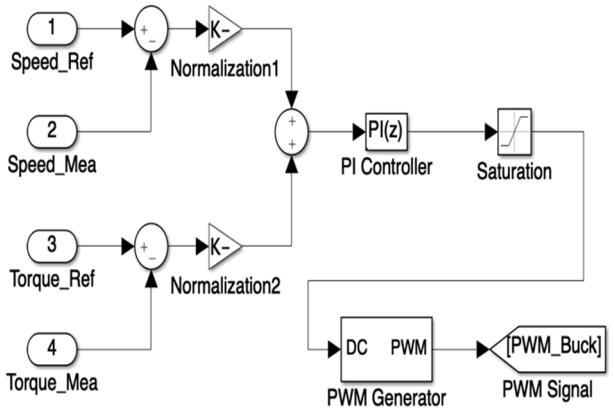

Fig. 6. PI controller for Buck converter to control of speed and torque

D. Energy Storage System

A hybrid electric ship is presented for the simulation. There are three generator engines and one ESS is feeding the DC grid of the vessel as Fig. 7. Battery modules for shipboard applications comprise the ESS.

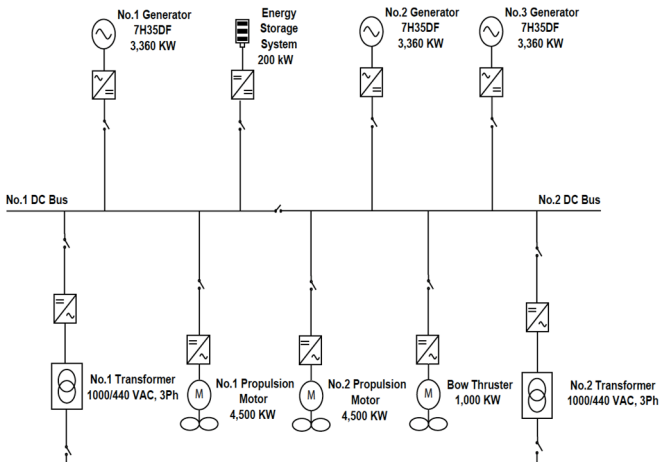

Fig. 7. Electric single line diagram for a proposed hybrid electric ship

The parameters being used for the ESS model are listed in table 1.

TABLE I. SPECIFICATION OF ENERGY STORAGE SYSTEM MODEL

No.	Parameters		
	Description	*Value*	*Unit*
1	Type	Lithium-Ion	
2	Nominal voltage	500	V
3	Rated capacity	400	Ah
4	Initial state-of-charge	80	%
5	Cut-off Voltage	375	V
6	Nominal discharge current	173.91	A
7	Capacity at nominal voltage	361.74	Ah

E. Mechanical Torque Induced to Motor

As mentioned in A. Engine Cranking Torque and Speed, in this paper, we set the speed reference of the motor in accordance with engine starting curve characteristics. With the speed reference, it is possible to generate the mechanical load torque induced to the motor by the equation (6). Be noted that the gear ratio between engine flywheel gear and starting motor gear should be considered here for the generation of the reference torque and speed.

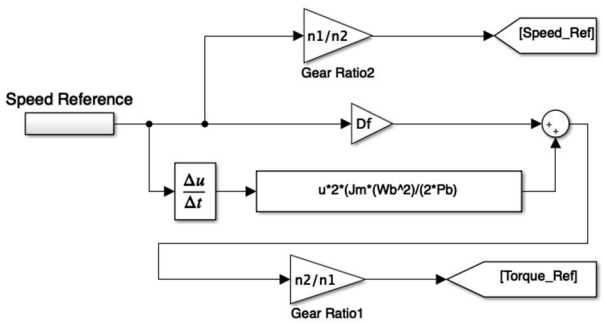

Fig. 8. Torque reference generation from speed reference

III. CONTROL OF ENERGY STORAGE SYSTEM

Main power generation engines are always equipped with the energy sources which enable the minimum three consecutive starting attempt for an emergency case such as blackout of the ship [14]. Therefore, the energy storage management system should secure the required energy for the engine to start. Once the main power generation is recovered, the main power generated can be fed to energy storage system for charging, Buck-Boost converter control in line with energy management system can be hired for discharging and charging of the ESS.

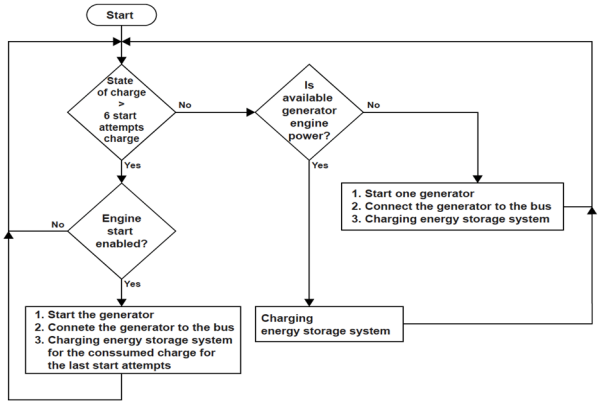

Fig. 9. Control strategy for engine starting and ESS

To keep the charge status of ESS beyond the charge status level for three consecutive start attempts, the state of charge should always be monitored and maintained up to the charge level for six consecutive start attempts, and after the start of the generator, it is recommended to charge the ESS for the amount of charge that is used for engine starting.

The energy-based control scheme suggested in [15] can be utilized for charging and discharging of the ESS, in the same context that the engine starting system is the load subsystem.

IV. SIMULATION RESULT

With the real engine parameters, the engine starting simulation is carried out with Matlab Simulink. During the engine start, the battery supplies the required charges to the motor through the power converter. The state of charge of the battery has been reduced to drive the engine flywheel, however, the amount of consumed can be retrieved in short term, because the generator begins to produce energy to grids, which is likely enough to reimburse the consumed amount of charges in the battery. It is notable that the used rated power of the engine is 3,360 kW in the simulation model.

TABLE II. SPECIFICATION OF ENGINE AND MOTOR USED IN THE SIMUATION MODEL

No.	Parameters		
	Description	*Value*	*Unit*
1.1	Engine Type	7H35DF	
1.2	Inertia (Engine + Alternator)	1421.8	$kg \cdot m^2$
1.3	Engine Speed	720	rpm
1.4	Engine Rated Power	3,360	kW
2.1	Motor Type	Wound Field DC motor	
2.2	Motor Rated Power	75	HP
3	Gear Ratio	25	

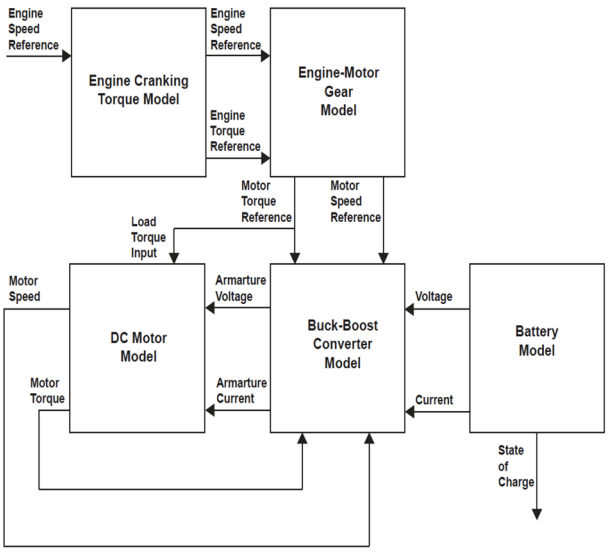

Fig. 10. Simulation model

The PI controller equipped the Buck-Boost converter controlled the voltage and current of the armature to follow the cranking speed reference.

Fig. 11. Motor speed simulation result

To increase the speed of the engine against the load torque from the engine flywheel, a substantial amount of current are supplied from the battery. However, the capacity of a common battery system in hybrid ships is sufficiently large enough for the concerned energy level.

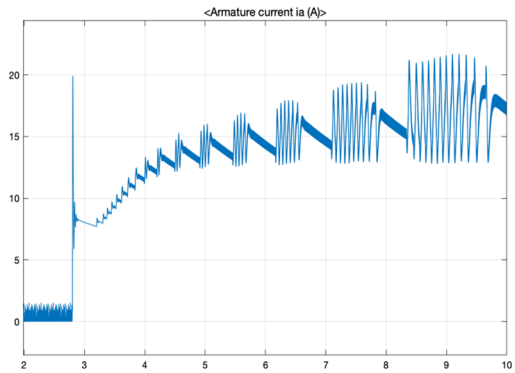

Fig. 12. Armature current supplied from the battery

Less than 0.03% of charge is depleted for an attempt to single generator to start through an efficient motor control strategy.

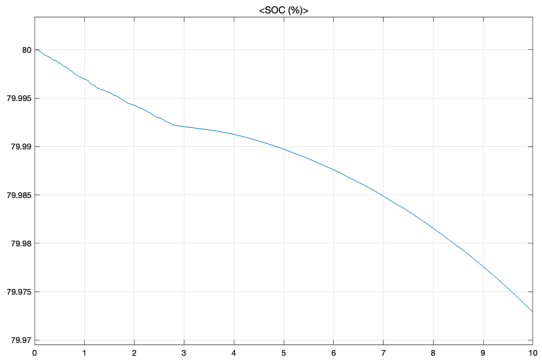

Fig. 13. Battery State of Charge during engine starting (%)

V. EXPERIMENTAL RESULT

Test is done to validate battery capacity, power of motor to start the HiMSEN 9H21/32 engine as Fig. 14. Two 24Vdc electric motors are installed on the engine for the experiment. The other motor is installed on the other side of engine. The motor starter and battery panel are located beside of the engine as Fig. 15. The specification of engine and motor used for the ESS model are listed in table 2.

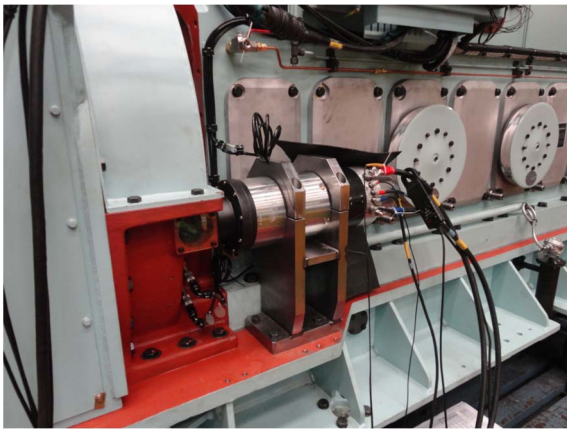

Fig. 14. View of the DC starting motor mounted on 9H21/32 engine

Fig. 15. Motor starter and battery panel

TABLE III. SPECIFICATION OF ENGINE AND MOTOR USED IN THE EXPERIMENT

No.	Parameters		
	Description	***Value***	***Unit***
1.1	Engine Type	9H21/32	
1.2	Inertia (Engine + Alternator)	521.8	$kg \cdot m^2$
1.3	Engine Speed	900	rpm
1.4	Engine Rated Power	1,800	kW
2.1	Motor Type	Wound Field DC motor x 2	
2.2	Motor Rated Power	15 x 2	kW
3.1	Battery Type	Lead-Acid	
3.2	Battery Volatge	24	V
3.3	Battery Capacity	1000	Ah

The voltage and current of battery modules are measured as Fig. 16. The engine is started successfully for consecutive six engine starting. Although, after six consecutive starting, the voltage of battery is dropped from 24Vdc to 17 Vdc due to the lack of battery capacity: 24 kWh, it is notable that normal ESS capacity onboard these days is ten times larger. Furthermore, considering the size of 1,800 kW engine, installing of minimum 200 kWh of ESS is reasonable to be installed onboard in a practical manner. Therefore, the starting system with ESS onboard and 24Vdc motors are considered an appropriate substitute of conventional pneumatic starting system.

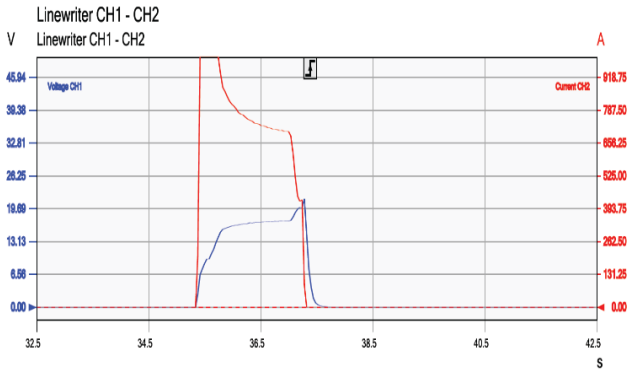

Fig. 16. Motor voltage and current during the start phase

VI. FURTHER DISCUSSIONS

Besides the engine starting system, there still exists pneumatic equipment dependent systems on internal combustion engines. Those systems can be replaced with electric devices in the same manner, particularly, it is encouraging to note that their power consumption is much less than the starting system.

For example, most diesel engines have pneumatic emergency stop equipment, normally requires 7~10 bar of air supply. The device is a short-term and single-purpose actuating instrument in comparison with the engine starting system mostly covered in this paper. In that regard, here we present one of the available substitutes, and they are purely electrical activated type, already have proven its reliability for construction types of machinery, e.g., forklift trucks. These DC solenoid oriented devices can be applied as an effective fuel cut off the device in combination with an appropriate linkage arrangement between governor and cylinder fuel pumps.

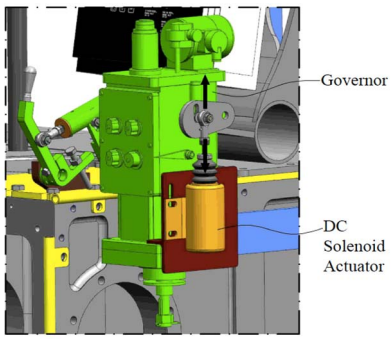

Fig. 17. Emergency stop device power by DC solenoid

VII. CONCLUSION

In this paper, an electric auxiliary system and the related control system for an internal combustion engine have been proposed. The proposed approach can reduce the capital cost of the vessel by eliminating the compressed air system including compressors, air tanks, valves, air filters, pressure reducer, and relevant pipes. And also the operator can save operational cost upon maximizing the usage of ESS.

The main concerned issue in the conversion of the existing pneumatic power to a new electric power device is how to get the required power without bringing any chance of fault or damaging system reliability. The simulation result shows that a converter-controlled DC motor combined with ESS drives the engine starting motor to the cranking speed. The charge consumed is less than 0.1% of the ESS for a single start and it can be charged within seconds after the started generator begins to supply electric power to the grid.

The proposed design could be challenging for the engine manufacturers and shipbuilders in the sense of the system re-design. However, considering the benefits provided by the hybrid-electric propulsion and the fact that the ESS is already available in a hybrid electric ship, it is highly worthwhile to invest in the electric auxiliary system on internal combustion engines for both engine manufacturer, shipbuilders and ship-owners.

REFERENCES

[1] M. K. Zadeh, R. Gavagsaz-Ghoachani, S. Pierfederici, B. N. Mobarakeh and M. Molinas, Stability analysis of hybrid AC/DC power systems for More Electric Aircraft, IEEE Applied Power Electronics Conference and Exposition (APEC'16), 2016.

[2] Torstein I. Bø, Andreas R. Dahl, Tor A. Johansen, Eirik Mathiesen, Michel R. Miyazaki, Eilif Pedersen, Roger Skjetne, Asgeir J. Sørensen, Laxminarayan Thorat, and Kevin K. Yum, Marine Vessel and Power Plant System Simulator, IEEE Access, 2015.2496122

[3] Torstein I. Bø, Dynamic Model Predictive Control for Load Sharing in Electric Power Plants for Ships, Modeling of Hybrid Marine Electric Propulsion Systems, Norwegian University of Science and Technology June 2012.

[4] Roy Nilsen, Electrical Drives, Norwegian University of Science and Technology 2018.

[5] M. K. Zadeh, R. Gavagsaz-Ghoachani, J-P. Martin, S. Pierfederici, B. N. Mobarakeh and M. Molinas, Discrete-Time Tool for Stability Analysis of DC Power Electronics-Based Cascaded Systems, IEEE Transactions on Power Electronics, vol.32, no.1, pp.652-667, 2017.

[6] J. Linares-Flores and H. Sira-Ramirez, DC motor velocity control through a DC-to-DC power converter, Proc. Of the 43rd IEEE Conf. pn Decision & Control, Paradase Island, Bahamas, pp.5297-5302, 2004.

[7] F. Antritter, P. Maurer and J. Reger, Flatness based control of a buck-converter driven DC motor, Proc. Of the 4th IFAC Symposium on Mechatronic Systems, Heidelberg, Germany, pp.1-6, 2006.

[8] H. El Fadil and F. Giri, Accounting of DC-DC power converter dynamics in DC motor velocity adaptive control, Proc. Of IEEE International Conf. on Control Applications, Munich, Germany, pp.3157-3162, 2006

[9] M. A. Ahmad, R. M. T. R.Ismail and M. S. Ramli, Control strategy of Buck converter driven DC motor: A comparative assessment, Australian Journal of Basin and Applied Sciences, vol.4, no.10, pp.4893-4903, 2010.

[10] R. Sureshkumar and S. Ganeshkumar, Compartive study of proportional integral and backstepping controller for buck converterm Proc.of International Conference on Emerging Trends in Electrical and Computer Technology, Tamil Nadu, India, pp.375-379, 2011.

[11] H. Sira-Ramirezand M. A. Oliver-Salazar, On the robust control of buck-converter DC-motor combinations, IEEE Trans. Power Electronics, vol.28, no.8, pp.3912-3922, 2013.

[12] J. Linares-Flores, A. Orantes-Molina and A.Antonio-Garcia, Smooth starter for a DC machine through a DC to DC Buck converter, Ingenieria Investigacion y Tecnologia, vol.12, no.2, pp.137-148, 2011

[13] Victor Manuel Hernandez-Guzman, Ramon Silva-Ortigoza, and Daniel Munoz-Carrillo, International Journal of Innovative Computing, Information and Control Volume 11, Number 2, April 2015.

[14] Rules for classification: Ships — DNVGL-RU-SHIP Pt.4 Ch.8. Edition January 2018.

[15] M. K. Zadeh, L. M. Saublet, R. Gavagsaz-Ghoachani, S. Pierfederici, B. N. Mobarakeh and M. Molinas "Energy management and stabilization of a hybrid DC microgrid for transportation applications", IEEE Trans- actions on Power Electronics, vol.32, no.1, pp.652-667, 2017

[16] Hyundai Heavy Industries: HIMSEN H21/32 Project Guide